# Quantifying the effects of spatial resolution on the mesoscale modelling of the Dutch storm of 1953

By

Qidi Yu

**Additional thesis**
in Geoscience and Remote Sensing

at the Delft University of Technology

| | | |
|---|---|---|
| Supervisor: | Dr. Sukanta Basu, | TU Delft |
| Thesis committee: | Prof. dr. Simon Watson, | TU Delft |
| | Dr. Stephan de Roode, | TU Delft |

TU Delft

# Contents

## Abstract

The Weather Research and Forecasting (WRF) model is used to investigate the horizontal spatial resolution sensitivity by simulating the 1953 Dutch storm, the grid sizes are 27, 9, 3, 1, 0.5 km from domain 1 to domain 5 respectively. Overall, the the probability density functions of wind speed of all time do not show higher resolution corresponding to higher maximum wind speed and more possibility to detect stronger winds. Because finer resolution domains feature a relatively weak model of wind intensity than coarser resolution domains. In the case, simulations are used two PBL scheme, YSU and Shin-Hong scheme. Three measurement stations with historical meteorology observation in 1953 are selected, Schiphol Netherlands, Leeuwarden Netherlands and Bentwaters United Kingdom. By comparison the measured data and all simulated data, the result from Shin-Hong scheme at the inner domain (d05) perform the best wind speed.

# 1 Introduction

Disastrous weather process is a significant part of meteorology for human beings, such as heavy wind and severe rain. Most this kind of process come with casualties and property loss. Thus, it is important to improving predictive accuracy.

Numerical weather predictions (NWPs) as a tool to provide predictions on many atmospheric elements. Three-dimensional primitive equation models, for instants the Weather Research and Forecasting (WRF) has used to simulate severe wind events. Nowadays, with the development of computing power, mesoscale atmospheric models are able to run at fine resolutions.

In earlier studies of resolution sensitivity, Gentry and Lackmann (2010) did a sensitivity test of simulating tropical cyclone structure, they used grid spacing from 8 km – 1 km, 4 km is the best resolution for eyewall structure, features within the eyewall start to be resolved from 2km, and only at 1 km resolution, updraft and downdraft cores within the lower levels of the eyewall are partially resolved. Bryan and Morrison (2012) use three different horizontal resolution 4 km, 1 km and 0.25km, the most realistic simulation come from $\Delta x = 0.25km$. Then come to 2013 (Sun, Y. et al., 2013), horizontal resolution sensitivities of a tropical cyclone at gray-zone resolution (7.5 – 1 km) are tested, there is a significant increase in tropical cyclone intensity as the resolution increase from 3 km to 1 km, and they use four different convective parameterization schemes, the best performance scheme at highest resolution show a better simulation results in terms of storm intensity and structure. In 2018 (Xu, H., Wang, Y. and Wang M., 2018), they represent convective boundary layer (CBL) turbulence by numerical models to investigate the effect of scale-dependent PBL scheme, the results show simulation results with the gray-zone scheme was closer to observations.

According to these results from different case studies, resolution sensitivity and model sensitivity by scale-dependent PBL scheme are worth to be further evaluated. In this case, we are focus on the Dutch storm from 1953.

# 2 Case study

The Dutch storm of 1953 was considered here, which occurred from 31st January to 1st February 1953 in the North Sea region, especially the whole east coast of Scotland and England to the coast of Netherlands. This specific case is interesting because it's one of the most devastating historical storm in Netherlands during twenty-century. About 2000 people were drowned by the rapid raised surge, some 1600 from Netherlands and 350 is in England from the records of that time (Lamb, H., 1991).
During that time, the strong winds over the North Sea region, as we can see from Figure 1, a direct northerly cold airstream came from the Arctic and reached Shetland in the Northern Isles of Scotland. The central pressure was 968 hPa at a point midway between northwest Scotland and south Norway at 12h on the 31st. At same time an anticyclone was building up on Atlantic and moving to the east. On the 1st of February, it centered at near blue circle (56°N 15°), the central pressure was 1034 hPa. After 12 hours, it moved to southeast of Germany, and the central pressure decreased to only 984 hPa. As a consequence, the storm was involved marked a very sharp change of weather in Britain and on the European plain. According to observation of the storm, the strongest pressure gradient was shown around the North Sea center, and a strongest gust of 109 knots (56.1 m/sec) was measured between 9 and l0 h on the 31st by an anemometer on Costa Hill, Orkney (red point in Figure 1).

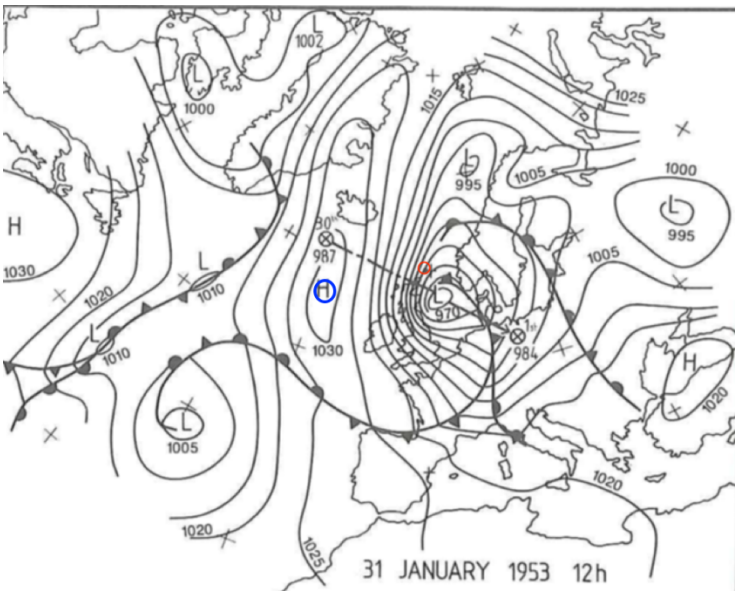

Figure 1. weather chart of 31 January 1953 12UTC (Lamb, H., 1991)

# 3 Literature review

## 3.1. Gray-zone PBL

The numerical weather prediction (NWP) simulates planetary boundary layers (PBLs) turbulence over domains spacing from several hundred meters to the entire global, there are two broad classes of modelling. For the larger domains, they are called mesoscale modelling, as for the smaller domains, large-eddy simulation (LES) is defined. How to classify them, it mainly depends on the value $l/\Delta$, the ratio of the size of energy-containing $l$ and the scale of the spatial filter $\Delta$. As Figure 2 shows, in mesoscale limit,

$\Delta_{meso} \gg l$ ,then the value of ratio $l/\Delta$ is far more less than 1. Therefore, in these models, there is no turbulence resolved, only mean flows are computed. In large-eddy simulation (LES), it is in the inertial subrange $\Delta_{LES} \ll l$ which is the value of ratio $l/\Delta$ is much more than 1. It's a three-dimensional PBL schemes parameterization. That's the reason why the energy- and flux-containing turbulence is resolved (Wyngaard,2004). Table 1 shows their main differences.

In Figure 2, there is a range called 'terra incognita' as an intermediate area between mesoscale and LES. Traditionally, this range's resolution used in severe storms with partial grid scale and partial subgrid scale, which belongs to the gray zone (Hong and Dudhia 2012). Thus, on the gray zone, not all the turbulence can be resolved. The subgrid scale turbulence parameterization become a difficult part for the resolution of gray zone. Thanks to the development of computing power, gray-zone modelling can be realized. Shin and Hong demonstrate that the nonlocal transports determine the scale dependency of total subgrid scale transport (Shin and Hong,2013).

In the WRF model, the physics options for the PBL scheme options, it has 15 options in total. In this case, the first option YSU scheme as a benchmark and the eleventh option Shin-Hong scheme are used. Table 2 show the details of these simulations.

Table 1. different based on grid size.

| Coarse grid spacing | Fine grid spacing |
|---|---|
| PBL schemes are defined as $\Delta \gg l$ | LES schemes are defined as $\Delta \ll l$ |
| All eddies are sub-grid | All major eddies are resolved |
| 1D column schemes handle sub-grid vertical fluxes | 3D turbulence schemes handle sub-grid mixing |

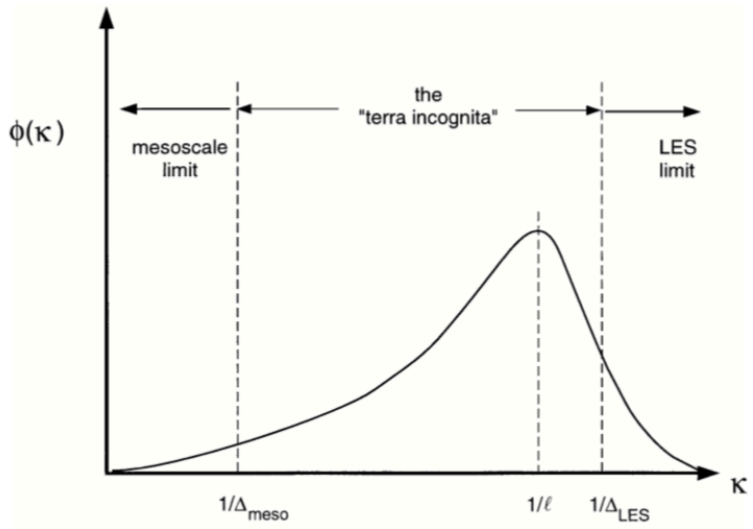


Figure 2. The turbulence spectrum $\phi(\kappa)$ as a function of wavenumber $\kappa$ (Wyngaard,2004).

Table 2. detail of this case's runs.

| Number of simulation | Number of domain | Resolution [km] | Number of using core | Scheme option | Simulation time |
|---|---|---|---|---|---|
| Run 1 | 5 | 27,9,3,1,0.5 | 32 | YSU | 9 days |
| Run 2 | 5 | 27,9,3,1,0.5 | 32 | Shin-Hong | 9 days |

## 3.2. The YSU Scheme

The Yonsei University(YSU) PBL utilize a nonlocal turbulent coefficient to account for vertical transportation, it's a the first-order closure scheme (Hong and Lim, 2006). For the mixing layer ( $z \le h$ ), the equation of a variable C of its diffusion is

$$\frac{\partial C}{\partial t} = \frac{\partial}{\partial z}\left[ K_c\left(\frac{\partial C}{\partial z} - \gamma_c\right) - \overline{(w'c')}_h \left(\frac{z}{h}\right)^3 \right] \qquad \dots (1)$$

where $K_c$ is the diffusivity coefficient of eddy and $\gamma_c$ is a correction term for local gradient, which takes the total flux including large-scale eddies part into account, the inversion layer flux is $\overline{(w'c')}_h$ , z is the height, $\frac{\partial}{\partial z}\left[ K_c\left(\frac{\partial C}{\partial z} - \gamma_c\right)\right]$ is the vertical diffusion term which contains the nonlocal convective eddies mixing, h is the top level of turbulence mixing disappeared and t is time. Above the mixing layer (z > h), a local diffusion method is used to compute diffusion at free atmosphere, which use $K_m$ to calculate local eddy diffusivity.

$$K_m = \kappa \omega_s z \left(1 - \frac{z}{h}\right)^p \qquad \dots (2)$$

where p is the profile shape exponent which chosen to be 2, $\kappa$ is equal to 0.4 and it is called the von Karman constant, $\omega_s$ is the velocity scale number at top of surface layer, z is the distance from the surface, and h is the boundary-layer height (Hong, et al., 2006).

## 3.3. The Shin-Hong Scheme

The Shin-Hong PBL scheme based on YSU scheme designed for sub-kilometer transition scales. The term 'gray-zone' in this scheme is defined as vertical transportations that is resolved and parameterized are studied at resolution between 4 km and 25m in convective boundary layers. The gray zone of a physical process in numerical models is defined as the range of model resolution where the process is partly resolved and partly parameterized (Shin and Hong, 2012). The Shin-Hong PBL scheme is a scale-aware scheme (Shin and Hong,2013). The subgrid-scale (SGS) turbulent transport profile is parameterized, which is resolution-dependent. In nonlocal PBL schemes, parameterize nonlocal and local transportations are separated based on their difference of scale dependency.

For the parameterizations of the SGS nonlocal transport, at resolution $\Delta$ , is modeled by multiplying a grid-size dependency function and total nonlocal transport profile.

$$<\omega'\theta'>^{s(\Delta_*),NL} = <\omega'\theta'>^{NL} P_{NL}(\Delta_{*cs}), \qquad \dots (3)$$

$$P_{NL}(\Delta_{*cs}) = 0.243 \frac{\left(\Delta_{*cs}\right)^2 + 0.936\left(\Delta_{*cs}\right)^{\frac{7}{8}} - 1.110}{\left(\Delta_{*cs}\right)^2 + 0.312\left(\Delta_{*cs}\right)^{\frac{7}{8}} + 0.329} + 0.757, \qquad \dots (4)$$

where $<\omega'\theta'>^{NL}$ is the total nonlocal transport profile, the superscripts S is SGS and NL is nonlocal, $\Delta_{*cs} \equiv \Delta / C_{cs} z_i = \Delta_* / C_{cs} (\Delta_* = \Delta / z_i)$ and $z_i$ is the height of PBL and $C_{cs}$ is a stability function, the term $P_{NL}(\Delta_{*cs})$ is the grid-size dependency function of the SGS nonlocal heat transport and an empirical function fit into the reference data for a free-convection case (Hong and Dudhia 2012).

As for the parameterizations of local heat transport, the eddies diffusivity functions are used.

$$< \omega'\theta' >^{s(\Delta_*),L} = -K_H(\Delta_*)\frac{\partial\overline{\theta^{\Delta}}}{\partial z} = -K_{H,PBL}P_L(\Delta_*)\frac{\partial\overline{\theta^{\Delta}}}{\partial z}, \quad \ldots (5)$$

$$P_L(\Delta_*) = 0.280\frac{(\Delta_*)^2 + 0.870(\Delta_*)^{\frac{1}{2}} - 0.913}{(\Delta_*)^2 + 0.153(\Delta_*)^{\frac{1}{2}} + 0.278} + 0.720. \quad \ldots (6)$$

where $K_H$ is the vertical diffusivity, the superscript L is local and H is heat, $K_{H,PBL}$ is the vertical diffusivity used in conventional PBL. The term $P_L(\Delta_*)$ is the grid-size dependency function of the SGS local heat transport.

For this $K_{H,PBL}$, the K-profile in the YSU scheme is chosen:

$$K_{H,PBL} = \kappa\omega_s z\left(1-\frac{z}{h}\right)^2 \quad \ldots (7)$$

where $\kappa$ is the von Karman constant which is equal to 0.4, $\omega_s$ is mixed-layer velocity scale. The bulk Richardson number is equal to zero at the PBL height h (Shin and Hong, 2015).

## 3.4. Published results of comparing YSU and Shin-Hong scheme

According to a study of representing convective boundary layer turbulence by WRF model with different PBL parameterizations (H. Xu, Y. Wang and M. Wang 2018). As a comparison between YSU scheme and Shin-Hong scheme, two results are showed as following.

Figure 3a is the simulation result of power spectra of $\omega$ at 3 km on the innermost domain with resolution 0.333 km at 1400 BJT, 1 July 2016 at the Taklimakan Desert. As we can see, the Shin-Hong experiment show a result of power spectra quite close to the result of LES, but the YSU PBL show a clear underestimation of resolved energy.

Figure 3b is the results of PBL height at Tazhong station, using the GPS observation data compare with three simulation results. At the first four hours, the simulated heights are same. After that, YSU scheme provides the highest value, and the maximum height of YSU, Shin-Hong and GPS are 5850m, 5750m and 5200m respectively, both of them overestimate the turbulent mixing in unstable condition.

In summary, the Shin-Hong PBL improves the modelled simulations compared to the YSU scheme.

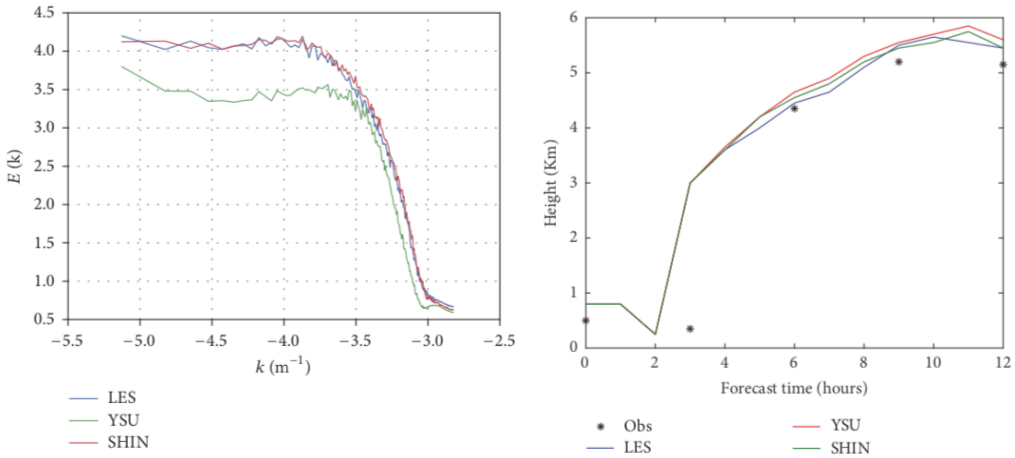


Figure 3a: Power spectra of *w* at 3000 m simulated on the d04 at 1400 BJT, 1 July 2016 (left), Figure 3b: Time series of the PBL height (units: km) over Tazhong station from the GPS sounding (black), LES (green), YSU (red), and Shin-Hong (blue) experiments (right), (H. Xu, Y. Wang and M. Wang 2018).

# 4 Model setups

In this case, a flexible and computationally-efficient platform, the Weather Research and Forecasting (WRF) Model Version 3.9.1.1, provides a wide range of meteorological applications across scales from hundreds of meters to dozens of thousands of meters, and includes numerous atmospheric physics parameterizations and advanced data assimilation modules.

During this simulation, a configuration consists of nested five-domain centered over the North Sea which is our target region, the outermost domain (d01, domain size: $3240km \times 2700km$ ) utilizes 27 km as grid size, and the innermost domain (d05, domain size: $334.5km \times 429.5km$ ) with a horizontal grid spacing of 0.5 km. Between d01 and d05, three domains are set, from outer to inner, grid spacing are 9 km, 3 km and 1km (Figure 4). For the vertical direction, 51 levels are used. The time steps setting for each domain are 180, 90, 30, 10, 5s for domain 1 to domain 5. The nesting method is one-way nesting which is no return to their parent domain.

In this selected case study, the setting of physics parameterizations is showing as Table 3. Two schemes are used, the planetary boundary layer (YSU) scheme and the Shin-Hong scheme, in order to identify the sensitivity of resolution.

The initial and boundary conditions from the ECMWF's atmospheric reanalysis of the 20th Century, ERA-20C (spatial resolution: 125 km; temporal resolution: 3 h) dataset, which does not provide the best estimate of the atmospheric state for the better observed period since 1979, were used for both the WRF simulations. The WRF model-generated profiles of wind speed started at 12 UTC on 30 January 1953 and continued for 48 hours. The WRF model output was stored every hour for a comprehensive analysis.

Table 3. Physics options setting

| | | |
|---|---|---|
| Physics | Surface-layer | Revised MM5 Monin-Obukhov shceme |
| | Microphysics | WSM 5-class scheme |
| | Radiation | RRTMG scheme (SW &LW) |
| | PBL | YSU<br>Shin-Hong |
| | Land surface | Unified Noah |

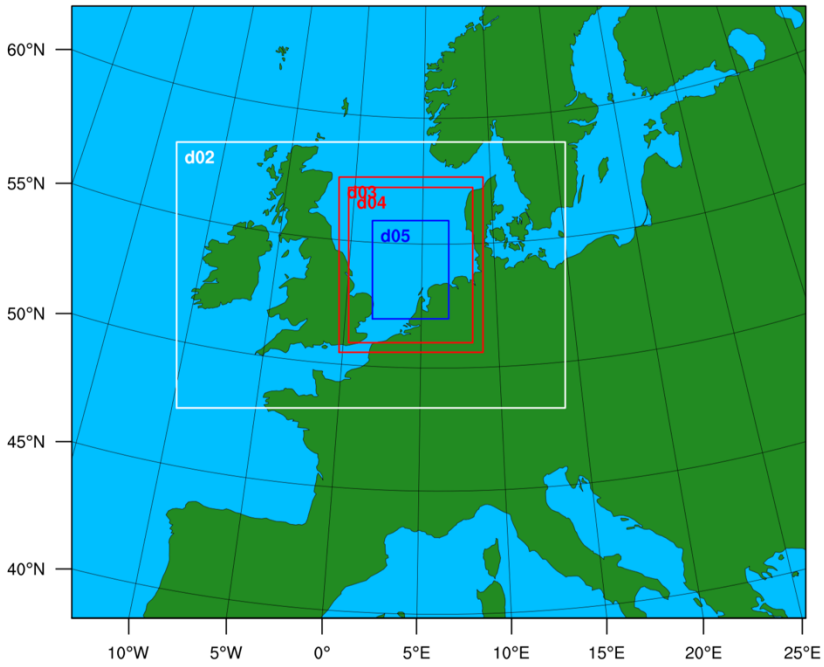

Figure 4: domain configuration

# 5 Results and discussion

## 5.1. Statistics results

In this case, calculated the probability density function (PDF) and cumulative distribution function (CDF) of wind speed for the entire simulation time series, in order to obtain the probability distribution of each domain from two PBL schemes. The purpose of this study is to figure out that with resolution increase, how do the wind speeds which are obtained change? A simply hypothetic result is that there will be detected larger maximum wind speed and higher probability of strong wind, with resolution increasing. Figure 5a and 5b show the wind speed PDF and CDF by the YSU results, Figure 6a and 6b show the wind speed PDF and CDF by the Shin-Hong results. The YSU result and Shin-Hong result are quite similar, because Shin-Hong PBL based on YSU designed, it's for sub-kilometer transition scales (200 m – 1 km). For the wind speed PDF of YSU, in the range of about 0 m/s - 10 m/s and 20 – 24 m/s, domain 3,4,5 have slightly higher probability, but for the rest domain 1 and 2 have higher possibility especially after 25 m/s which is the Beaufort scale 10 that is storm level wind. This is opposite to original expectation. As for the wind speed PDF of Shin-Hong, before 20 m/s, there is no clear difference for all domains, same situation for after roughly 27 m/s. But between approximately 20 – 23 m/s, domain 3,4,5 have a higher possibility, domain 1 and 2 show obvious high possibly from 23 – 27 m/s. This is inverse to the expectation as well. For the sake of finding the reason that case these phenomena, the next step is to consider terrain effect and model spin up time effect.

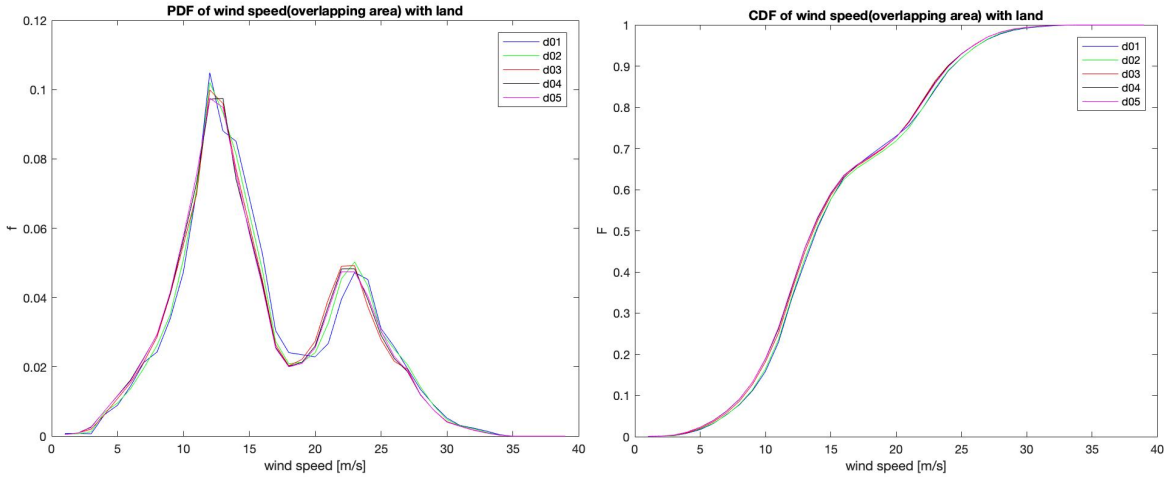


Figure 5a: PDF of wind speed at the overlapping area with d05 by using YSU scheme (right).
Figure 5b: CDF of wind speed at the overlapping area with d05 by using YSU scheme (left).

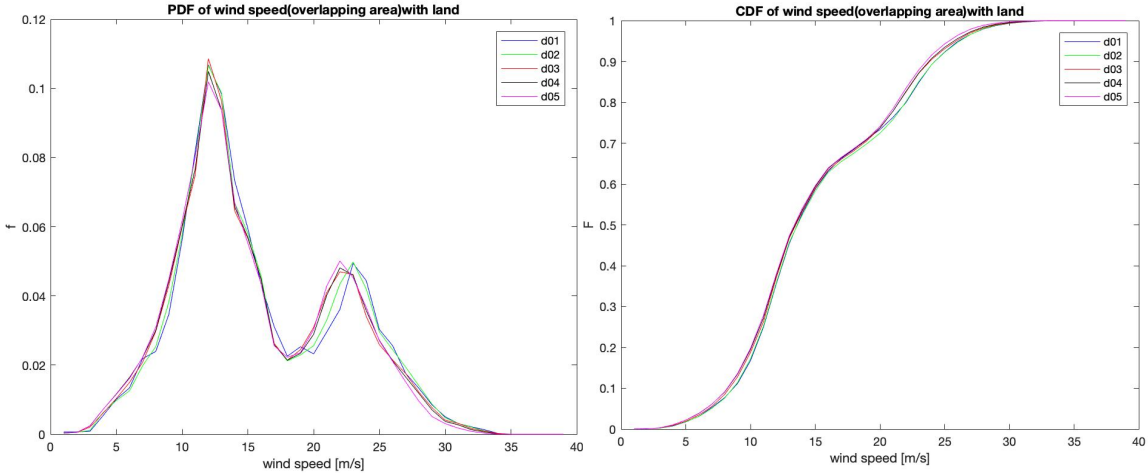


Figure 6a: PDF of wind speed at the overlapping area with d05 by using Shin-Hong scheme (right).
Figure 6b: CDF of wind speed at the overlapping area with d05 by using Shin-Hong scheme (left).

Only offshore data are selected, and use the data from the thirteenth hour to the end. Figure 7a, 7b show the wind speed PDF without land and subsequent thirty-six hours' data. However, only in the range of about 20 m/s to 24 m/s, finer resolution domain has more possibility. Even in the result of Shin-Hong scheme, domain 1 and 2 with slight higher PDF value from 24 – 26 m/s. Therefore, the effect of terrain and model spin up time not play an important role in domain variation of wind speed simulations.

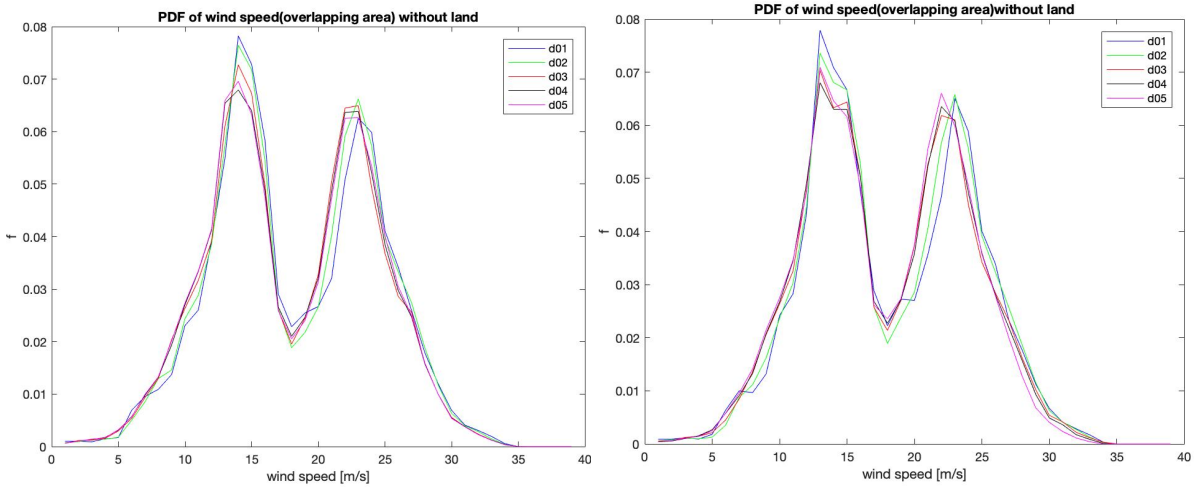


Figure 6a: PDF of offshore wind speed at the overlapping area with d05 by using Shin-Hong scheme from thirteen hours to the end (right).
Figure 6b: CDF of offshore wind speed at the overlapping area with d05 by using Shin-Hong scheme from thirteen hours to the end (left).

## 5.2. 2D map at specific moments

For the purpose of finding reasons of unexpected statistic results, Figure 8a, 8b show the five-domain simulated wind speed at the region of domain 5 at three moments: January 31st 6UTC, January 31st 18UTC and February 1st 6UTC which present from the storm start to developed to the storm dissipated. From the coarser resolution to the finer resolution, it's easy to notice that clearer images are provided, at same time we can find the reason for the PDF results. The wind speed become weaker for the inner domains, especially during the dissipation process. If we assume finer domain is closer to reality, coarser domains overestimate the wind speed.

Compare the result of YSU (Figure 8a) and Shin-Hong (Figure 8b), most of them are same, but for domain 4 and 5 with resolution 1 km and 0.5 km respectively, which belong to gray-zone resolution, there are several differences with each other (black circles). For January 31st 18UTC, the outcome of Shin-Hong shows a slight different patient at the edge of high wind speed area meeting with low wind speed area. As for February 1st 6UTC, Shin-Hong scheme detects some lower speed among the storm belt.

Although the initial conditions of the inner domains are interpolated by the outer domains, the performance is different. But back to our assumption, is the higher resolution increasing the accuracy of simulated wind speed?

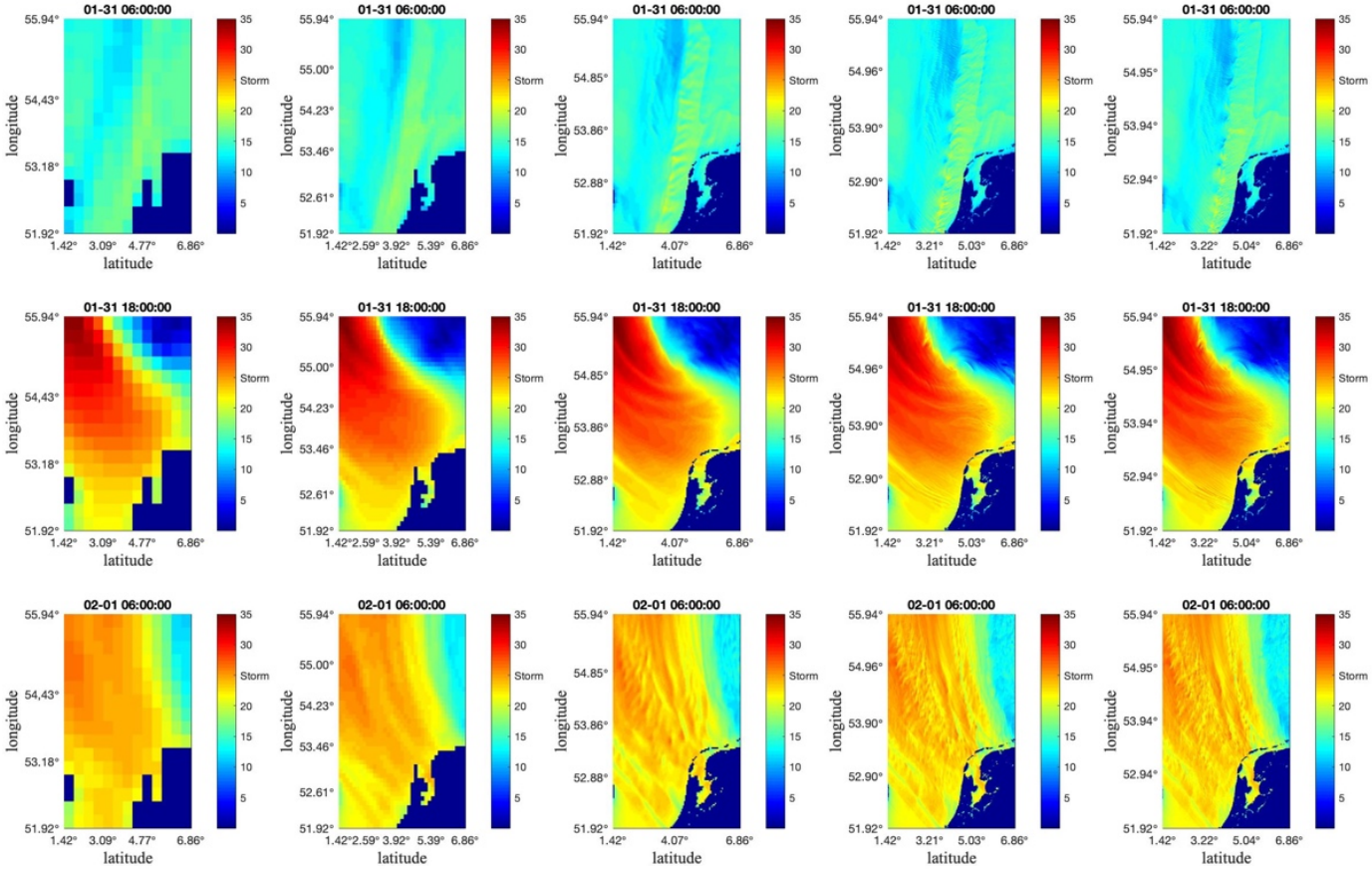


Figure 8a: 2D maps of YSU scheme at January 31st 6UTC (top five), January 31st 18UTC (middle five), February 1st 6UTC (bottom five).

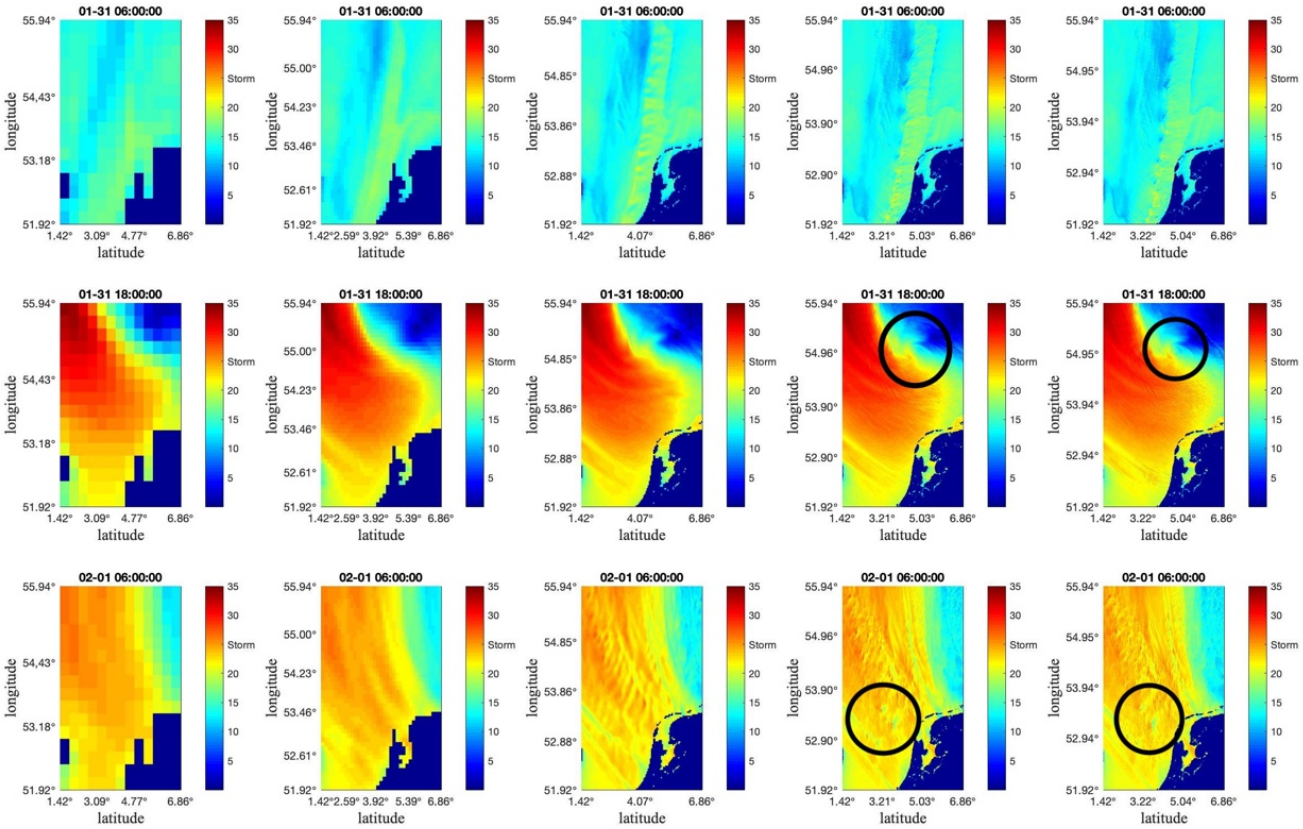


Figure 8b: 2D maps of Shin-Hong scheme at January 31st 6UTC (top five), January 31st 18UTC (middle five), February 1st 6UTC (bottom five).

## 5.3. Comparison with observation data

There are three stations' historical wind speed records ('Weather Spark', n.d.): Schiphol Netherlands (52.3092N, 4.7608E), Leeuwarden Netherlands (53.2034N, 5.7913E) and Bentwaters United Kingdom (52.3895N, 0.5375E). Their locations show on Figure 9a, 9b and 9c.

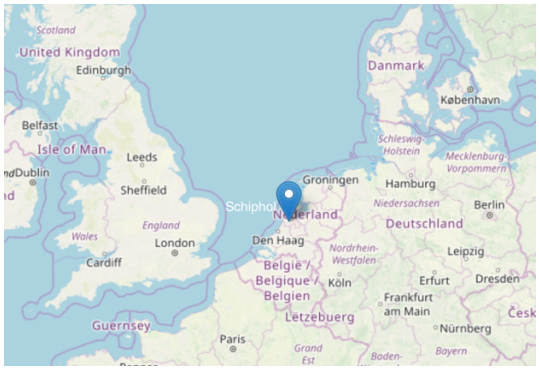


Figure 9a: location of Schiphol, Netherlands


Figure 9b: location of Leeuwarden, Netherlands

Figure 9c: location of Bentwaters, United Kingdom

Figure 10a,10b show the simulated wind speed by YSU and Shin-Hong scheme respectively and measured wind speed at station Schiphol from January 31st 0UTC to February 1st 12UTC. As we can see, simulation results from all domain are underestimated. From Figure 10a, we can see simulated wind speed values of domain 1 are most closer to observed values, which exceed the second closer result domain 5 during the night time. But for the daytime, domain 5 that has highest resolution performs better. By comparison, the domain 5 outcome of Shin-Hong scheme show almost all time perform the best, except in the afternoon of January 31st. In additional, the wind speed changing trend of the Shin-Hong scheme result at 0.5 km resolution is the most similar with observation.

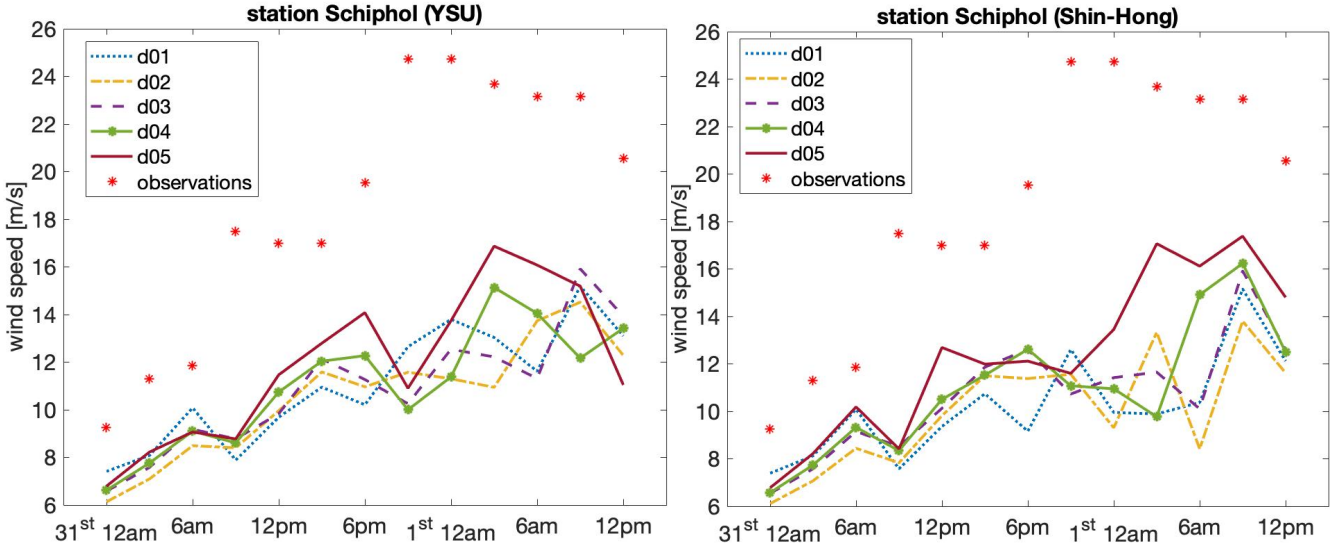





Figure 10a: YSU scheme results of all domains and observation at station Schiphol, during January 31st 0UTC to February 1st 12UTC (right)
Figure 10b: Shin-Hong scheme results of all domains and observation at station Schiphol, during January 31st 0UTC to February 1st 12UTC (left)

Figure 11a,11b are observed wind speed data and the simulated wind speed by YSU and Shin-Hong scheme respectively at station Leeuwarden from January 31st 0UTC to February 1st 12UTC. Almost all simulation results from all domain are underestimated before approximately January 31st 15UTC. Another noticeable is at February 1st 0UTC and 3UTC, wind speed rise suddenly, all of them underestimate the maximum wind speed which is near 35 m/s. For the simulation of YSU scheme, though, the data from domain 1 before January 31st 18UTC is the closest one to observation, but after that time, the trend of wind speed variation is totally opposite with observation. For the suddenly rise wind speed moment, domain 5's outcome provides closest value even it's still quite a lot underestimate the speed. The result of Shin-Hong performs better than that of YSU, in particular at domain 5, the variation trend compare with observation is the most similar except the suddenly increase part.

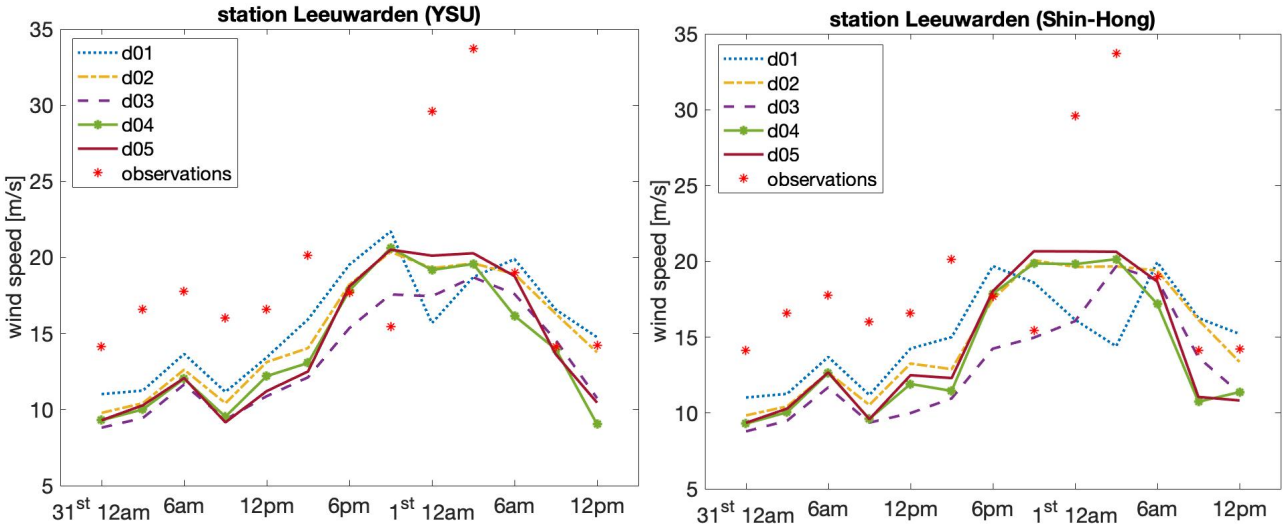


Figure 11a: YSU scheme results of all domains and observation at station Leeuwarden, during January 31st 0UTC to February 1st 12UTC (right)
Figure 11b: Shin-Hong scheme results of all domains and observation at station Leeuwarden, during January 31st 0UTC to February 1st 12UTC (left)

Comparison plots of station Bentwaters are presenting on Figure 12a, 12b. This point is a special one, it's not include in domain 5. Therefore, only other four domain outcomes and observation. The simulations are not like another two stations, it's not overestimate or underestimate too much compare with measured data. All the simulations show opposite variation trend during January 31st morning which is between January 31st 6UTC to January 31st 12UTC. After that, domain 3 and 4 results are closer to observations both of two PBL schemes. At this station, Shin-Hong scheme did not perform too much better than YSU, one possible reason is due to the inner domain with resolution 1 km instead of 0.5 km, but at some moments the simulation of Shin-Hong scheme is closer to reality, for example at February 1st 3UTC and 6UTC.

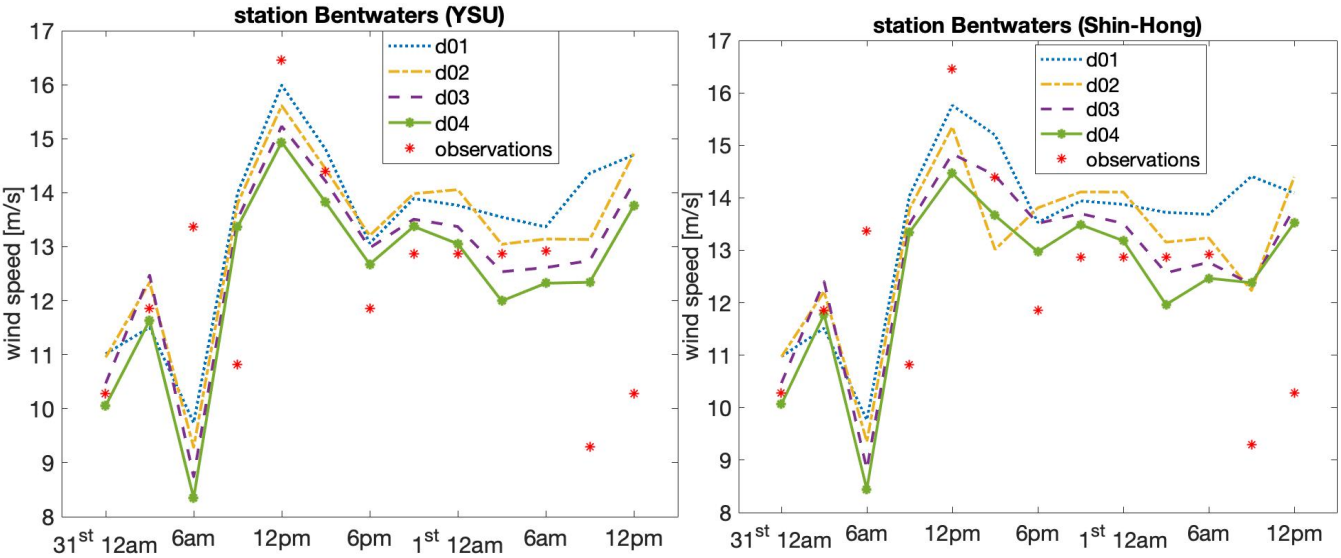


Figure 12a: YSU scheme results of all domains and observation at station Bentwaters, during January 31st 0UTC to February 1st 12UTC (right)
Figure 12b: Shin-Hong scheme results of all domains and observation at station Bentwaters, during January 31st 0UTC to February 1st 12UTC (left)

To summaries, the results of resolution sensitivity in this study show that the higher resolution simulation outcomes performed better than the coarser resolution. Additionally, the results of using Shin-Hong PBL scheme at the gray-zone resolution show more accuracy then others. However, at a specific area, inner domain outcomes do not detect more high wind speed value than outer domains statistically. This is not to say finer resolution not helpful, instead most of time the result of coaster resolution overestimate the

values. Moreover, the outer domain has more chance to have a total opposite variation trendy of wind speed compare with observation data.

# 6 Conclusions and future work

In this study, a series simulations of 1953 Dutch storm are conducted. In order to find resolution sensitivity of WRF model and the effects of using different parameterizations for the planetary boundary layer (PBL), which is to investigate the model sensitivity. These simulations use five domains from 27 km to 0.5 km, which including gray-zone resolution. As for the PBL setting, YSU scheme and Shin-Hong scheme are used that Shin-Hong scheme is designed for gray-zone which is resolution between 200m to 1 km.
The simulated results of wind speed from YSU scheme and Shin-Hong scheme both show the best simulation at the highest resolution (0.5 km), and Shin-Hong scheme at this resolution range perform better than that of YSU scheme, no matter the wind speed value or the variation tendency. That is to say it does improve the accuracy of simulation results.
However, the simulation results of gray-zone are not exactly match with observation, especially when the wind speed rise suddenly and dramatically. This means there are still some uncertainties for gray-zone simulation need to improve in the future. In this case, we only consider different PBL schemes, it will be a challenge to take other atmospheric physics options into account, for example shortwave and longwave radiation in fine scales. Besides, cumulus scheme is only active when dx > 5 km. So, it is turned off for domain 3, 4 and 5. For these domains, a key challenge is modeling across the gray zone to convection-permitting resolutions (Gao et al., 2017). Thus, do parametrization for corresponding event is good for better performance results. Moreover, the case of 1953 Dutch storm is a quite old event, there are not many existent meteorological observation records at that time, especially for the maritime observation. For the future work of resolution sensitivity, a case with more measured data is more helpful. At same time, higher resolution model (smaller than 500 m) can be used for the future studies.

# Bibliography

[1] Bryan, G. H. and Morrison H., Sensitivity of a Simulated Squall Line to Horizontal Resolution and Parameterization of Microphysics, American Meteorological Society, 140, 202-225 (2012).

[2] Gao, Y., L. R. Leung, C. Zhao, and S. Hagos, Sensitivity of U.S. summer precipitation to model resolution and convective parameterizations across gray zone resolutions, J. Geophys. Res. Atmos., 122, 2714–2733 (2017).

[3] Gentry, M. S. and Lackmann, G. M., Sensitivity of Simulated Tropical Cyclone Structure and Intensity to Horizontal Resolution, American Meteorological Society, 138, 688-704 (2010).

[4] H.H. Shin and S.-Y. Hong, Analysis of resolved and parameterized vertical transports in convective boundary layers at gray-zone resolutions, Journal of the Atmospheric Sciences, vol. 70, no. 10, pp. 3248–3261 (2013).

[5] Hong, Song–You, Yign Noh, Jimy Dudhia, A new vertical diffusion package with an explicit treatment of entrainment processes. Mon. Wea. Rev., 134, 2318–2341 (2006).

[6] Hong, S.-Y., and J. Dudhia, Next-generation numerical weather prediction: Bridging parameterization, explicit clouds, and large eddies. Bull. Amer. Meteor. Soc., **93,** ES6– ES9 (2012).

[7] Hubert Lamb. Historic Storms of North Sea, British and Northwest Europe, 1991.

[8] Shin, H. H., and S.-Y. Hong, Representation of the subgrid-scale turbulent transport in convective boundary layers at gray-zone resolutions. Mon. Wea. Rev., 143, 250-271 (2015).

[9] Sun, Y., L. Yi, Z. Zhong, Y. Hu, and Y. Ha, Dependence of model convergence on horizontal resolution and convective parameterization in simulations of a tropical cyclone at gray-zone resolutions, J. Geophys. Res. Atmos., 118, 7715–7732 (2013).

[10] S.-Y. Hong and J.-O. J. Lim, The WRF single-moment 6- class microphysics scheme (WSM6), Journal of the Korean Meteorological Society, vol. 42, no. 2, pp. 129–151 (2006).

[11] Weather Spark. (n.d.). Retrieved from https://weatherspark.com/h/d/147997/1953/2/1/Historical-Weather-on-Sunday-February-1-1953.

[12] Wyngaard, J. C., Toward numerical modeling in the ‘‘terra incognita.’’ J. Atmos. Sci., 61, 1816–1826 (2004).